Payri, R.; Tormos, B.; Salvador, FJ.; Araneo, L. (2008). Spray droplet velocity characterization for convergent nozzles with three different diameters. Fuel. 87(15-16):3176-3182. https://doi.org/10.1016/j.fuel.2008.05.028

Published as: Payri, Raul; Tormos, Bernardo; Salvador, Francisco Javier; Araneo, Lucio; (2008). Spray droplet velocity characterization for convergent nozzles with three different diameters. Fuel, 87, 15-16, 3176-3182. DOI: 10.1016/j.fuel.2008.05.028

DROPLET VELOCITY CHARACTERIZATION FOR THREE CONVERGENT NOZZLES WITH DIFFERENT DIAMETERS

R. Payri (*)(1), B. Tormos (1), F. J. Salvador (1), L. Araneo (2)

(1) CMT-Motores Térmicos, Universitat Politècnica de València

Cami de Vera s/n, E-46022 Spain.

(2) Politecnico di Milano, Dipartimento di Energetica, via La Masa 34

20156 Milano, Italy

(*) Corresponding author:

Dr. Raul Payri, rpayri@mot.upv.es

CMT-Motores Térmicos, Universitat Politècnica de València

Cami de Vera s/n, E-46022 Spain.

Telephone: +34-963879658

FAX: +34-963877659

Published as: Payri, Raul; Tormos, Bernardo; Salvador, Francisco Javier; Araneo, Lucio; (2008). Spray droplet velocity characterization for convergent nozzles with three different diameters. Fuel, 87, 15-16, 3176-3182. DOI: 10.1016/j.fuel.2008.05.028

ABSTRACT

On a direct injection engine the spray formation is the main determining factor over the quality of the air-fuel mixture and the subsequent combustion. This is the reason why it is of great importance to obtain and intimate understanding of the processes that take place during this very short time event. The core of the present work consists of the phase-Doppler anemometry non-intrusive measurements performed in various points of Diesel direct injection sprays in order to obtain the local speed of fuel droplets. The application of this technique to Diesel sprays is challenging and has certain limitations imposed firstly by the high droplet number concentration and secondly by the droplets typical high velocity and small size. The main objective is to perform extensive sets of measurements on convergent nozzles with various orifices diameters and internal geometries, observe and justified the differences and compare the experimental data with a theoretical approach derived by the authors in a previous work. This comparison helped to shed light over the reliability of the measurements performed.

KEY WORDS:

Diesel spray, fuel droplets velocity, injection, momentum flux.

Published as: Payri, Raul; Tormos, Bernardo; Salvador, Francisco Javier; Araneo, Lucio; (2008). Spray droplet velocity characterization for convergent nozzles with three different diameters. Fuel, 87, 15-16, 3176-3182. DOI: 10.1016/j.fuel.2008.05.028

NOMENCLATURE

$C\ (x, r)$	Mass concentration in the coordinate (x, r) of the spray.
$C_{axis}\ (x)$	Mass concentration in the coordinate x of the spray's axis.
i	Counter of Taylor's series
k-factor	Conicity factor
L	Orifice length
$\dot{M}_o$	Momentum flux at the nozzle outlet orifice.
$\dot{m}_f$	Fuel mass flux.
m_f	Fuel mass.
m_a	Air mass.
P_{back}	Backpressure.
P_{inj}	Injection pressure.
D	Mass diffusivity.
r	Radial coordinate.
R	Radius of the spray.
S	Spray tip penetration.
Sc	Schmidt Number.
t	Time.
$U_{axis}\ (x)$	Velocity in the coordinate x of the spray's axis.
U_o	Orifice outlet velocity.
$U\ (x, r)$	Axial velocity in the coordinates (x, r) of the spray.
x	Axial coordinate.

Published as: Payri, Raul; Tormos, Bernardo; Salvador, Francisco Javier; Araneo, Lucio; (2008). Spray droplet velocity characterization for convergent nozzles with three different diameters. Fuel, 87, 15-16, 3176-3182. DOI: 10.1016/j.fuel.2008.05.028

GREEK SYMBOLS:

α	Coefficient of the Gaussian radial profile for the axial velocity.
ϕ_i	Inlet diameter of the nozzle's orifice.
ϕ_o	Outlet diameter of the nozzle's orifice.
ρ_a	Ambient density.
ρ_f	Fuel density.
$\rho\ (x, r)$	Density in the coordinates (x, r) of the spray.
ν	Viscosity.
π	Pi number.
θ_u	Spray cone angle.

1. INTRODUCTION

Although sprays are commonly used in many industrial applications their study has always been difficult due to the complex phenomena involved. This complexity is accentuated in the particular case of sprays in direct injection Diesel engines because of the high frequency transient operation and the small characteristic time and length (1 ms and 25 mm respectively). In such adverse conditions from the point of view of the experimentation, the spray characteristics that can be measured are very limited. The most typical measurements are spray tip penetration and spray cone angle [1][2] which are macroscopic characteristics, and droplet velocity and droplet diameter, which are microscopic features [3][4][5]. In general, macroscopic measurements are more reliable than microscopic ones and it would be interesting to discover how the formers relate to the latter's. One of the key parameter which relates microscopic and macroscopic characteristics of the spray is momentum flux. It is considered by several authors as one of the most important parameter governing the spray

dynamics [6]. The momentum flux brings together the effective flux velocity at the orifice outlet, the fuel density, and the effective diameter of the nozzles orifices.

In this paper, the non-intrusive measurements of phase-Doppler anemometry are performed in various points of Diesel direct injection sprays in order to obtain the local speed of fuel droplets. The application of this technique to Diesel sprays is challenging and has certain limitations imposed firstly by the high droplet number concentration and secondly by the droplets typical high velocity and small size. The main objective is to perform extensive sets of measurements on three convergent nozzles with various orifices diameters and internal geometries in order to establish relations-ships between geometry and spray dynamic. Experimental results are also compared with a theoretical model based on the conservation of momentum flux. The comparison of the measurements with model, allowed, on one hand, the validation of the model in a wide range of operating conditions and, on the other hand it helped to shed light over the reliability of the measurements performed.

As far as the structure of the paper is concerned, the article is divided in six parts. In section 2, the experimental methodology is described. In this section, the nozzles, the injection conditions for the experimental measurements and experimental facilities used for the investigation are described. In section 3 the relevant equations of the theoretical approach are summarized. Following, in section 4, results concerning spray momentum flux and droplet velocities in different axial and radial position are shown. The results are analyzed in section 5. Finally, in section 6, the most important conclusions of the work are drawn.

2. EXPERIMENTAL METHODOLOGY

The system used to deliver high-pressure fuel to the injector is a normal automotive production series common rail system adapted to laboratory use and featuring temperature

control. The system is constituted by a high pressure pump, able to reach up to 160 MPa, and a conventional rail with a pressure regulator. The injector employed is a Bosch second generation solenoid type. A Repsol CEC RF-06-99, with a density of 820.2 kg/m^3 and a kinematic viscosity of 2.67 mm^2/s (measured at 40ºC) was used as fuel in the experiments.

2.1 Nozzles

The tested nozzles were of the mono-orifice axi-symmetric type with average diameters varying between 107 and 149 μm. These nozzles have conical convergent orifice geometry with the same conicity level. The relevant data about the nozzles' internal geometry, summarized in Table 1, was obtained by injecting silicone inside and then studying with an electronic microscope the resulting moulds. This procedure is described by Macian et al in [7]. The conicity factor, *k-factor*, is given by the following formula: $k - factor = 100 \cdot \frac{\phi_i - \phi_o}{L}$, where ϕ_i and ϕ_o are the orifice inlet and outlet diameters respectively, and L is the orifice length, all expressed in μm.

2.2 Injection conditions for the experimental measurements.

For each nozzle there three injection pressures were used: 30, 80 and 130 MPa, and two ambient densities: 25 and 40 kg/m^3. It can be noticed that while the ambient densities cover the range encountered in a modern Diesel engine, the injection pressures employed are slightly lower. Furthermore, the main purpose of this work was to study the eventual tendencies, not to test the ultimate injection pressure that can be generated.

2.3 Momentum flux measurements.

As far as the momentum flux is concerned, a pressurized test rig with nitrogen is used. The measuring principle of this technique is explained in [6], and consists of measuring the impact force of the spray in a surface with a piezo-electric sensor. As long as the whole cross-section

of the spray is impacting on the sensor, this force is equal to the momentum flux at that cross-section. If the measurement position is close to the nozzle exit, the time evolution of the impact force is equal to the nozzle (hole) momentum flux, $\dot{M}_o$.

2.4 SF6 test rig and PDPA System.

The droplet velocity measurements have been performed in a pressurised test rig that offers better optical access than a normal engine but can still reproduce totally or partially the ambient conditions from the combustion chamber at the moment of the injection. The test rig is filled with a dense gas, sulphur hexa-fluoride (SF_6). Due to its high molecular mass it can reach the density values that normally occur in a Diesel engine at the moment of the injection (10 to 40 kg/m^3) at much lower pressures (0.2 to 0.5 MPa). The temperature inside the rig is constant, fixed at 25 º C. The rig is of the closed-loop type, which means that the gas is continuously circulated, passing rough filters that remove the injected fuel and then through the roots compressor that sends it back to the actual testing section.

The flow velocity next to the injector is lower than 2 m/s, so that it should not affect the diesel spray, while also avoiding window fouling. The rig is shown in Figure 1, where the system optics' location for the PDPA (phase Doppler particle anemometry) measurements is also shown. Details of the PDPA technique and system configuration are given in [5]. The geometrical points for taking measurements were divided in five sections at 25, 30, 35, 40 and 50 mm of axial distance from the orifice. Each section contained generally nine points with different radial distances that varied as a function of axial distance to orifice and ambient density.

Published as: Payri, Raul; Tormos, Bernardo; Salvador, Francisco Javier; Araneo, Lucio; (2008). Spray droplet velocity characterization for convergent nozzles with three different diameters. Fuel, 87, 15-16, 3176-3182. DOI: 10.1016/j.fuel.2008.05.028

3. SPRAY DYNAMIC: THEORETICAL APPROACH.

In order to rigorously impose momentum flux conservation in a Diesel spray, it is necessary to take into account the radial evolution of both, axial velocity and fuel concentration. For any section perpendicular to the spray axis in the steady region of a Diesel spray, momentum flux is conservative, and thus equal to that existing at the nozzle exit [6]. Consequently, the following equation can be written:

$$\dot{M}_o = \dot{M}(x) \tag{1}$$

where $\dot{M}(x)$ and $\dot{M}_o$ are the momentum flux through a spray cross section at a distance x and at the orifice outlet respectively. It can be assumed that the radial profile of the velocity at the nozzle exit is flat, and thus $\dot{M}_o = \dot{m}_f U_o$, where $\dot{m}_f$ is the mass flux, and U_o the orifice outlet velocity.

In order to develop expression (1), momentum must be integrated over the whole section:

$$\dot{M}_o = \dot{M}(x) = \int_0^R 2\pi\rho(x,r)\, r U^2(x,r)\, dr \tag{2}$$

where the x-coordinate coincides with the spray axis, and the r-coordinate is the radial position (perpendicular to the spray axis). In this expression $\rho(x,r)$ is the local density in the Diesel Spray, and $U(x,r)$ is the axial velocity.

The density at an internal point of the spray, taking into account the local concentration, can be written as:

$$\rho(x,r) = \rho_f \frac{1}{C(x,r)\left(1 - \frac{\rho_f}{\rho_a}\right) + \frac{\rho_f}{\rho_a}} \tag{3}$$

with ρ_f, the fuel density, ρ_a the air density and $C(x,r)$ the local fuel mass concentration, defined as:

Published as: Payri, Raul; Tormos, Bernardo; Salvador, Francisco Javier; Araneo, Lucio; (2008). Spray droplet velocity characterization for convergent nozzles with three different diameters. Fuel, 87, 15-16, 3176-3182. DOI: 10.1016/j.fuel.2008.05.028

$$C = \frac{m_f}{m_a + m_f} \tag{4}$$

with m_f the local mass of fuel, and m_a the local mass of air.

For the developed region in the spray, fuel concentration and axial velocity can be considered to follow a Gaussian radial profile [8]:

$$U(x,r) = U_{axis}(x) \cdot exp\left(-\alpha \left(\frac{r}{R} \right)^2 \right) \tag{5}$$

$$C(x,r) = C_{axis}(x) \cdot exp\left(-\alpha \cdot Sc \cdot \left(\frac{r}{R} \right)^2 \right) \tag{6}$$

with Sc the Schmidt number, and α the shape factor of the Gaussian distribution. The Schmidt number is the ratio of effective momentum diffusivity to effective mass diffusivity, and represents the relative rate of momentum and mass transfer, including both molecular and turbulent contributions. It is defined as:

$$Sc = \frac{\nu}{D} \tag{7}$$

with ν the viscosity, and D, the mass diffusivity.

The radius of the spray R, can be expressed with respect the spray cone angle as:

$$R = x \cdot \tan\left(\frac{\theta_u}{2} \right) \tag{8}$$

At this point it is necessary to point out that radial distributions of axial velocity are not well known in sprays. Some authors use gas jet distributions as a first approximation. Experimental similarities between them have been always remarked by other researchers ([1], [11], [12], [13]). Different expressions for radial profiles can be found in the literature ([9],[10], [12],[14]). Correas ([12]) made a comparative study of all them, and proposed a modification of the expressions by Hinze ([9]), which has been usually considered the profile that better fits the available experimental data in the literature. This profile has been adopted by the authors

in ([1][6]) and in the present work. As it will be seen in the following section, results obtained with PDPA system have shown that the Gaussian profile is a reasonable approach for the type of sprays within the scope of the present work.

Substituting Eqs. (3), (5) and (6) in Eq. (2) and integrating, the authors obtain the following expression for the spray momentum ([8]):

$$\dot{M}_o = \frac{\pi}{2\alpha}\cdot\rho_a\cdot\tan^2\left(\frac{\theta_u}{2}\right)\cdot x^2\cdot U_{axis}^2\cdot\sum_{i=0}^{\infty}\frac{1}{\left(1+i\frac{Sc}{2}\right)}\cdot\left[\left(\frac{U_{axis}}{U_0}\right)\left(\frac{1+Sc}{2}\right)\left(\frac{\rho_f-\rho_a}{\rho_f}\right)\right]^i \qquad (9)$$

Equation (9) can be simplified for the particular case of Sc=1 and by assuming that the fuel density is much higher than the ambient, and thus $\frac{\rho_f-\rho_a}{\rho_f}\cong 1$. With these assumptions, equation (9) becomes:

$$\dot{M}_o = \frac{\pi}{2\alpha}\cdot\rho_a\cdot x^2\cdot\tan^2\left(\frac{\theta_u}{2}\right)\cdot U_0\cdot\left[-U_{axis}-U_0 Ln\left(1-\frac{U_{axis}}{U_0}\right)\right] \qquad (10)$$

The authors ([8]) found that, for a given set of conditions, Schmidt number's variation between 0.6 and 1.4 did not have any significant influence on the calculated on-axis velocities for the spray region beyond approximately $20D_{eq}$ (with $D_{eq}=D_o\cdot\sqrt{\rho_f/\rho_a}$ as explained in [1]). The consequence is that when Sc is not known, which is the case, the simplified equation for Sc =1 can be expected to give very good estimations.

Another possible simplification refers to the consideration of a constant density in the chamber (and thus, inside the spray) equal to the air density in the injection chamber. According to [8], assuming that the density is constant inside the spray and equal to the ambient one, the equation (10) can be simplified further. In fact, if $\rho(x,r)=\rho_a$, the integration

Published as: Payri, Raul; Tormos, Bernardo; Salvador, Francisco Javier; Araneo, Lucio; (2008). Spray droplet velocity characterization for convergent nozzles with three different diameters. Fuel, 87, 15-16, 3176-3182. DOI: 10.1016/j.fuel.2008.05.028

of equation (2) simplifies and it leads to Equation (11) (the complete theoretical deduction can be found in Desantes *et al.* [1])

$$U_{axis} = \frac{\dot{M}_o^{1/2}}{\rho_a^{1/2} \cdot \left(\frac{\pi}{2\alpha}\right)^{1/2} \cdot x \cdot \tan\left(\frac{\theta_u}{2}\right)} \tag{11}$$

The authors ([8]) compared the velocity axial profiles calculated from equation (10) (constant density) and equation (10) (local density variations with Sc=1) and they found that the main differences occur very close to the orifice because in this initial part of the spray, the local density is far from the assumption of constant density. Nevertheless beyond $30D_{eq}$ the differences are less than 3% . This is due to the fact that the constant density assumption starts becoming valid as the jet develops and spreads apart.

4. EXPERIMENTAL RESULTS

4.1 Momentum flux results

As commented before, the spray momentum can be measured experimentally with good reliability and precision by simply employing a sensor that measures the impact force of the spray on a plate perpendicular to its axis [6]. The momentum values in stabilized conditions measured for all the nozzles and injection pressures are shown in Table 2. The backpressure was fixed to 2.5 bar.

As can be seen from the table, the highest momentum flux is found for N3, followed by N2 and finally by N1. Due to the fact that all nozzles have similar value for the k-factor definition (same conicity), no important differences in outlet velocity are expected, and the only

parameter that directly affects momentum is the outlet diameter. In fact, momentum flux can be expressed as:

$$\dot{M}_o = \dot{m}_f \cdot U_o \tag{12}$$

With $\dot{m}_f$ the instantaneous mass flow rate, and U_o the effective outlet velocity.

Taking into account mass conservation and Bernoulli's equation, equation (12) can be expressed as:

$$\dot{M}_o = \dot{m}_f \cdot U_o = C_a \cdot \frac{\pi \cdot \phi_o^2}{4} \cdot \rho_f \cdot U_o^2 \tag{13}$$

with C_a a contraction coefficient ([6]). As all the nozzles has the same nozzle k-factor value, the parameters C_a and U_o should not differ so much between them for a given injection condition, and so, differences in momentum flux between nozzles are mainly due to the different outlet diameter.

4.2 Velocity measurement results for on-axis locations

The velocity measurements obtained in the steady part of the spray, on-axis, for all nozzles and experimental conditions are presented in Figure 2. Each graph contains data from all nozzles at different injection pressures and ambient density conditions. At this point it is necessary to remark that measurements with PDPA are only possible with a high level of confidence under conditions where fuel concentration is not very high, and this is why the minimum axial position where measurements are taken is 25 mm. In general terms, it can be seen that, as expected and for a given nozzle the velocities decrease with the penetration distance and the ambient density, whiles increase with the injection pressure. As far as the influence of geometry is concerned, it can be observed that for a given condition (injection pressure and chamber density) and for a given position, the velocity in the axis is clearly lowest for N1. Differences between nozzle N2 and nozzle N3 are not so clear, but nevertheless

Published as: Payri, Raul; Tormos, Bernardo; Salvador, Francisco Javier; Araneo, Lucio; (2008). Spray droplet velocity characterization for convergent nozzles with three different diameters. Fuel, 87, 15-16, 3176-3182. DOI: 10.1016/j.fuel.2008.05.028

in general terms, it seems that N3 presents higher velocity in the axis than N2. This result could be explained by equation (11). In fact, as this equation expresses, for a given axial position, *x*, the velocity in the axis is directly proportional to the square root of momentum flux, $\dot{M}_o$, and inversely proportional to the tangent of the spray half angle. As it will be seen in section 5 and due to the fact that nozzles geometry in terms of k-factor are very similar, no important differences in terms of spray cone angle between nozzles should be expected and so, the differences reflected in Figure 2 would be mainly due to momentum differences observed in Table 2. In fact, in this table, momentum values for nozzle N2 are much closer to values of N3 than to those measured for Nozzle 1.

4.3 Velocity measurement results for different radial locations

In Figure 3, the radial distribution profiles for all nozzles and for an injection pressure of 30 MPa and a density of 40 kg/m^3 are depicted. Measurements have been taken at six axial locations measured from the nozzle orifice outlet: 25, 30, 35, 40, 45, 50 mm. For each axial position several measurements have been taken at different radial positions. As can be seen from the figures, the higher the axial position the higher the maximum radial position measured. This observation results obvious if it is considered the conical shape of the spray. In this Figure, the points obtained for the radial position, *r=0*, are those shown in Figure 1 (axial values). Typical Gaussian velocity profiles are obtained at each section. The level of correlation of these experimental profiles with the theoretical Gaussian profiles proposed in section 3 will be analysed in next section.

Published as: Payri, Raul; Tormos, Bernardo; Salvador, Francisco Javier; Araneo, Lucio; (2008). Spray droplet velocity characterization for convergent nozzles with three different diameters. Fuel, 87, 15-16, 3176-3182. DOI: 10.1016/j.fuel.2008.05.028

5. ANALYSIS OF THE RESULTS. COMPARISON WITH THEORETICAL MODEL

From the theoretical point of view and considering equation (10), apart from the spray momentum, the half spray cone angle $\theta_M/2$ is also needed for the model predictions. This parameter can be obtained from a fitting of the exponential function to the normalized profiles of axial velocity. For that purpose, the velocity fields measured with the PDPA system have been used. Figure 4 shows the velocity values normalized by the spray axis velocity plotted in terms of normalized coordinates (r/x) for different injection conditions. From these experimental points, a fit has been performed to the function $\exp(-k\,(r/x)^2)$ which has also been plotted in Figure 4. A good fit in the main part of the spray has been searched for, due to uncertainties in measurement velocities at the spray boundary. Taking into account equations (5) and (8), the fit constant k can be converted to obtain the experimental cone angle velocity. The figure demonstrates the validity of the Gaussian profiles for the velocity field. In fact, the level of fitting is quite high.

In tables 3, 4 and 5, the values of the spray cone angle (momentum spreading angle), obtained following the previous methodology, are shown for all injection conditions.

The values of spray angle from the table reflect what was said in section 4.2 about the similarity of spray cone angle as a result of having the nozzles almost the same level of conicity (k-factor).

Once all the necessary inputs for the model are available, Figure 5 shows the results of spray droplet velocity measured in the spray axis at different axial positions for all nozzles and all injection pressures and two densities (25 kg/m^3 and 40 kg/m^3). At this point it is necessary to remark that measurements with PDPA are only possible with a high level of confidence under

conditions where fuel concentration is not very high, and this is why the minimum axial position where measurements are taken is 25 mm. As stated before, at this distance, variations due to Schmidt number or local density variations are already negligible and so, the simplified equation (11) is enough in order to compare experimental results with those obtained experimentally. As can be seen from the figure, the agreement between the model and the experimental data is quite acceptable especially at low injection pressures.

6. CONCLUSIONS

In this work a wide set of experimental measurements of droplet velocity with the PDPA technique have been used in order to compare convergent nozzles of different diameter. Additional measurements of momentum flux and the support of a theoretical model previously derived were a fundamental help in order to explain the behaviour of results. From this work the following conclusions can be drawn.

- Experimental results of droplet velocity measured with the PDPA technique have been used in order to compare convergent nozzles with small differences in the level of conicity but with different outlet diameters.
- Axial velocities on-axis and at different radial positions have been measured.
- Higher velocity values have been observed for the nozzles with higher momentum.
- The comparison of experimental measurements with theoretical model has shown an acceptable agreement and so, measurements have been useful in order to validate the proposed theoretical approach for a wide injection conditions.

Published as: Payri, Raul; Tormos, Bernardo; Salvador, Francisco Javier; Araneo, Lucio; (2008). Spray droplet velocity characterization for convergent nozzles with three different diameters. Fuel, 87, 15-16, 3176-3182. DOI: 10.1016/j.fuel.2008.05.028

ACKNOWLEDGEMENTS

This research has been funded by "Vicerrectorado de Innovación, Desarrollo e Innovación de la Universidad Politécnica de Valencia" in the frame of the Project "Estudio del flujo en el interior de toberas de inyección Diesel", Reference Nº 3150.

REFERENCES

[1] Desantes, J.M., Payri, R., Salvador, F.J., Gil, A., "Development and validation of a theoretical model for Diesel spray penetration", Fuel, vol. 85, pp. 910-917, 2006.

[2] Payri, R., Salvador, F. J., Gimeno, J. Soare, V., "Determination of Diesel sprays characteristics in real engine in-cylinder air density and pressure conditions", J. Mech. Sci. Technol., vol. 19, pp. 2040-2052, 2005.

[3] Doudou, A., Maslouhi, A., 2007, Macro-microscopic investigation of high-pressure sprays injected by a common rail system. Journal of Mechanical Science and Technology, Vol 21, Issue 8, pp. 1284-1292

[4] Benajes. J., Payri. R., Molina. S., Soare. V., 2005. Investigation of the influence of injection rate shaping on the spray characteristics in a Diesel common rail system equipped with a piston amplifier, Journal of Fluids Engineering, Vol. 127, No.6 pp.1102-1110.

[5] Araneo, L., Soare V., Payri, R., Shakal, J., "Seting up a PDPA system for measurements in a diesel spray", J. Phys: Conf Ser 2006; 45: 85-93

[6] Payri, R., García, J. M., Salvador, F. J., Gimeno J., "Using spray momentum flux measurements to understand the influence of Diesel nozzle geometry on spray characteristics", Fuel, vol. 84, pp. 551-561, 2005.

[7] Macián, V., Bermúdez, V., Payri, R., Gimeno, J., "New technique for determination of internal geometry of a Diesel nozzles with the use of silicone methodology", Exp. Techniques; vol. 27, pp. 39-43, 2003.

[8] Desantes, J. M., Payri, R., García, J. M., Salvador, F. J., "A contribution to the understanding of isothermal Diesel spray dynamics", Fuel, vol. 86, pp. 1093-1101, 2007.

[9] Hinze, J.O., Turbulence. McGraw-Hill. ISBN 0-07-029037-7, 1975.

[10] Pastor, J.V., Encabo, E., Ruíz, S., New modelling approach for fast online calculations in sprays, SAE Paper 2000-01-0287, 2000.

[11] Naber, J.D., Siebers, D.L., "Effect of gas density and vaporization on penetration and dispersion of diesel sprays", SAE Paper 960034, 1996.

[12] Correas, D. "Theoretical and experimental study of isothermal diesel free sprays, PhD Thesis, Universidad Politécnica de Valencia, 1998 [in Spanish].

[13] Prasad CMV, Kar, S. "An investigation on the diffusion of Momentum and mass of fuel in a Diesel fuel Spray. ASME J Eng Power 1976: 1-11.76-DGP-1

[14] Abramovich, G., N., "The theory of turbulent jets", MIT Press; 1963, ISBN 0-262-01008-9.

Published as: Payri, Raul; Tormos, Bernardo; Salvador, Francisco Javier; Araneo, Lucio; (2008). Spray droplet velocity characterization for convergent nozzles with three different diameters. Fuel, 87, 15-16, 3176-3182. DOI: 10.1016/j.fuel.2008.05.028

LIST OF TABLES AND FIGURE CAPTIONS

Published as: Payri, Raul; Tormos, Bernardo; Salvador, Francisco Javier; Araneo, Lucio; (2008). Spray droplet velocity characterization for convergent nozzles with three different diameters. Fuel, 87, 15-16, 3176-3182. DOI: 10.1016/j.fuel.2008.05.028

Nozzle code	Inlet diameter [μm]	Outlet diameter [μm]	*k*-factor (conicity)
N1	128	107	2.1
N2	147	126	2
N3	167	149	1.8

Table 1. Tested nozzles main characteristics.

Published as: Payri, Raul; Tormos, Bernardo; Salvador, Francisco Javier; Araneo, Lucio; (2008). Spray droplet velocity characterization for convergent nozzles with three different diameters. Fuel, 87, 15-16, 3176-3182. DOI: 10.1016/j.fuel.2008.05.028

Spray Momentum M_o [N]		Nozzle		
		N1	N2	N3
Inj. Press. [MPa]	30	0.47	0.62	0.75
	80	1.32	1.61	1.83
	130	2.18	3.05	3.68

Table 2. Spray momentum measurements with 2.5 bar counter pressure.

Published as: Payri, Raul; Tormos, Bernardo; Salvador, Francisco Javier; Araneo, Lucio; (2008). Spray droplet velocity characterization for convergent nozzles with three different diameters. Fuel, 87, 15-16, 3176-3182. DOI: 10.1016/j.fuel.2008.05.028

θ_u [º] – Nozzle N1		Ambient Density [kg/m^3]	
		25	**40**
Inj. Press. [MPa]	**30**	19.8	23.02
	80	18.8	21.66
	130	18.2	21.14

Table 3. Spray cone angle for nozzle N1.

Published as: Payri, Raul; Tormos, Bernardo; Salvador, Francisco Javier; Araneo, Lucio; (2008). Spray droplet velocity characterization for convergent nozzles with three different diameters. Fuel, 87, 15-16, 3176-3182. DOI: 10.1016/j.fuel.2008.05.028

θ_u [º]– Nozzle N2		Ambient Density [kg/m^3]	
		25	**40**
Inj. Press. [bar]	**30**	19.7	21.6
	80	18.1	21.4
	130	17.4	21.6

Table 4. Spray cone angle for nozzle N2.

Published as: Payri, Raul; Tormos, Bernardo; Salvador, Francisco Javier; Araneo, Lucio; (2008). Spray droplet velocity characterization for convergent nozzles with three different diameters. Fuel, 87, 15-16, 3176-3182. DOI: 10.1016/j.fuel.2008.05.028

θ_u [º]– Nozzle N3		Ambient Density [kg/m^3]	
		25	**40**
Inj. Press. [bar]	**30**	18	20.7
	80	17.48	21.7
	130	17.4	21.6

Table 5. Spray cone angle for nozzle N3.

Published as: Payri, Raul; Tormos, Bernardo; Salvador, Francisco Javier; Araneo, Lucio; (2008). Spray droplet velocity characterization for convergent nozzles with three different diameters. Fuel, 87, 15-16, 3176-3182. DOI: 10.1016/j.fuel.2008.05.028

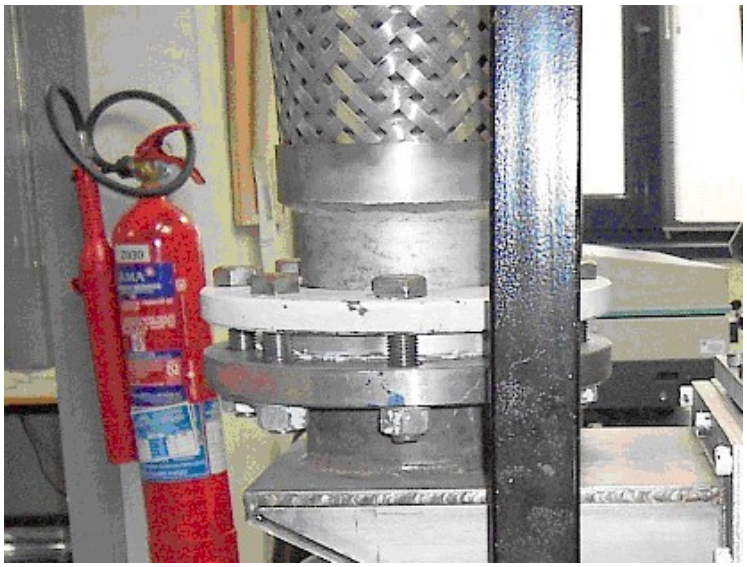

Figure 1. The set up, with the transmitting optic from the top, the receiving optic horizontal, the injector from the left in the scavenging flow.

Published as: Payri, Raul; Tormos, Bernardo; Salvador, Francisco Javier; Araneo, Lucio; (2008). Spray droplet velocity characterization for convergent nozzles with three different diameters. Fuel, 87, 15-16, 3176-3182. DOI: 10.1016/j.fuel.2008.05.028

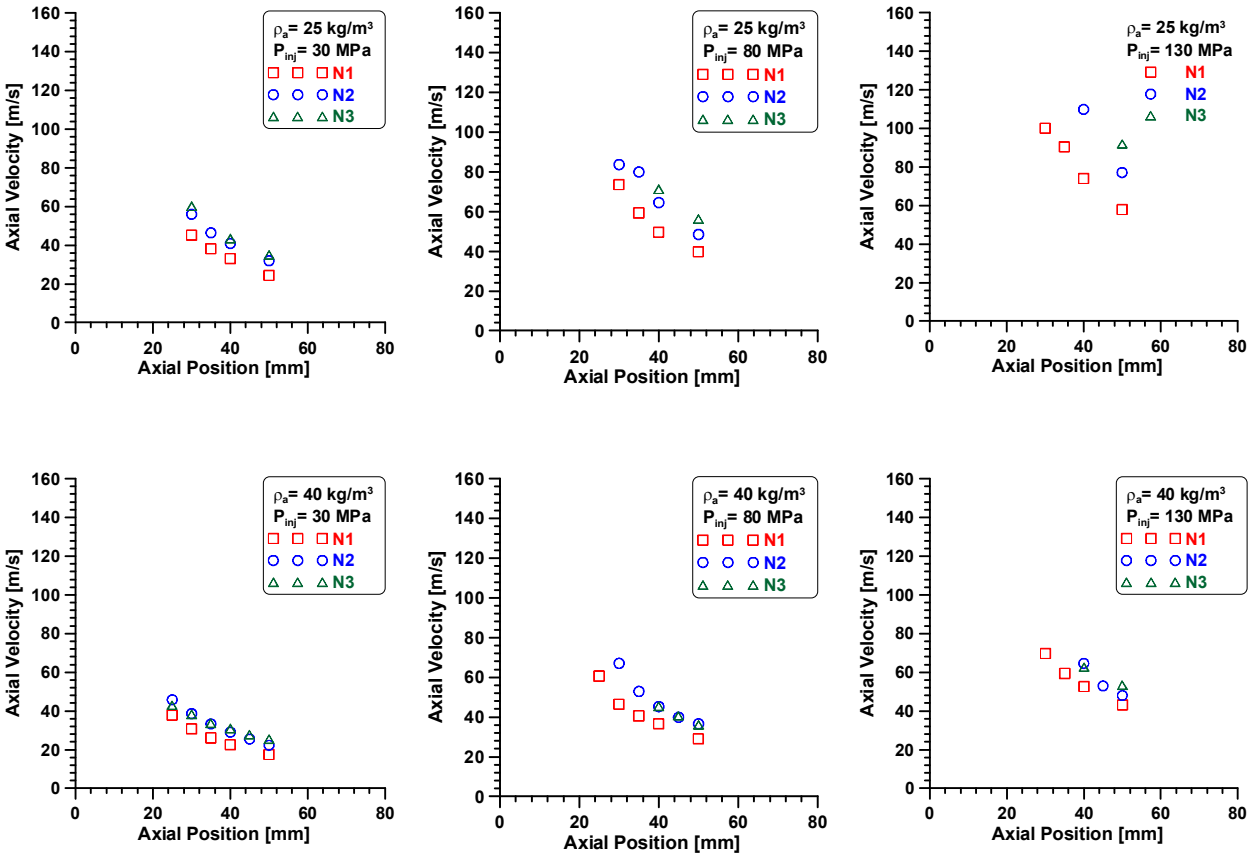

Figure 2. On-axis velocity measurements for all nozzles and conditions

Published as: Payri, Raul; Tormos, Bernardo; Salvador, Francisco Javier; Araneo, Lucio; (2008). Spray droplet velocity characterization for convergent nozzles with three different diameters. Fuel, 87, 15-16, 3176-3182. DOI: 10.1016/j.fuel.2008.05.028

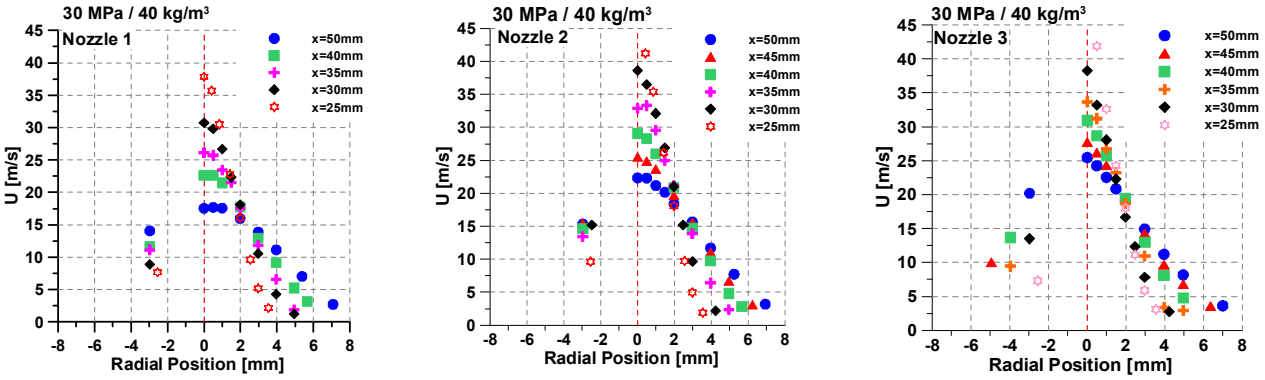

Figure 3. Velocity radial distribution profiles at different axial positions for all nozzles at P_{inj}=30 MPa and 40kg/m^3 ambient density.

Published as: Payri, Raul; Tormos, Bernardo; Salvador, Francisco Javier; Araneo, Lucio; (2008). Spray droplet velocity characterization for convergent nozzles with three different diameters. Fuel, 87, 15-16, 3176-3182. DOI: 10.1016/j.fuel.2008.05.028

N1

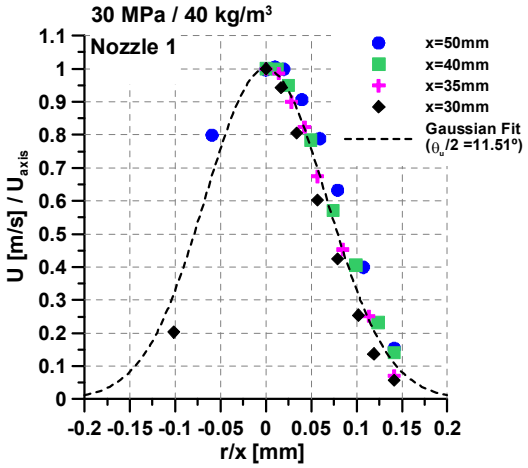

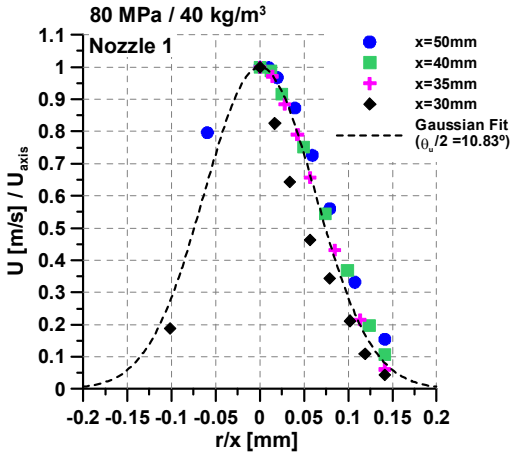

N2

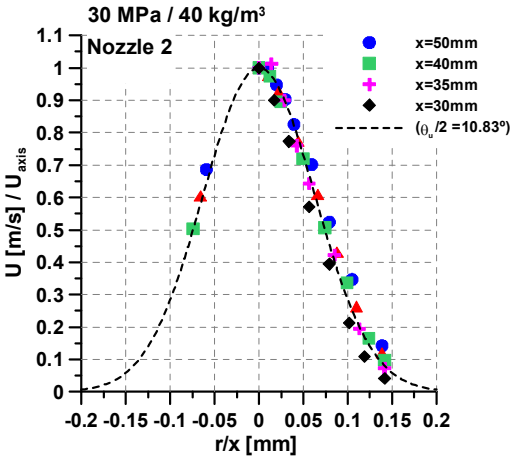

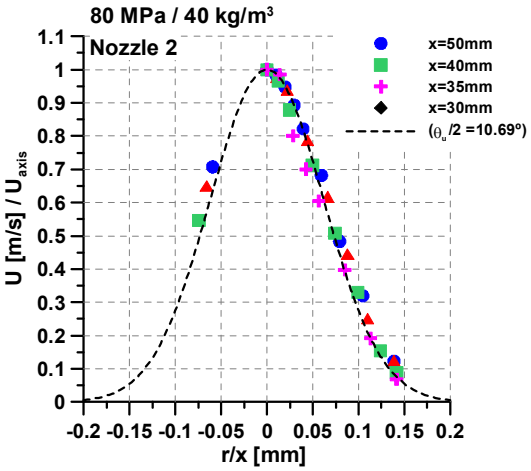

N3

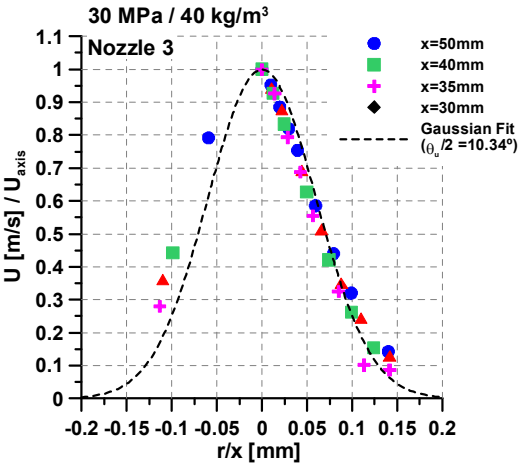

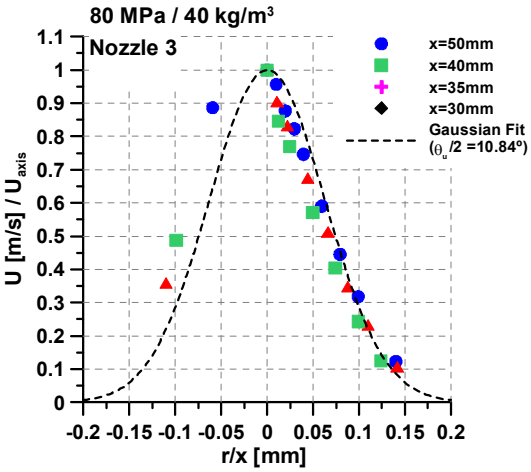

Figure 4. Experimental velocity profiles in different sections of the spray. Comparison with Gaussian profile.

Published as: Payri, Raul; Tormos, Bernardo; Salvador, Francisco Javier; Araneo, Lucio; (2008). Spray droplet velocity characterization for convergent nozzles with three different diameters. Fuel, 87, 15-16, 3176-3182. DOI: 10.1016/j.fuel.2008.05.028

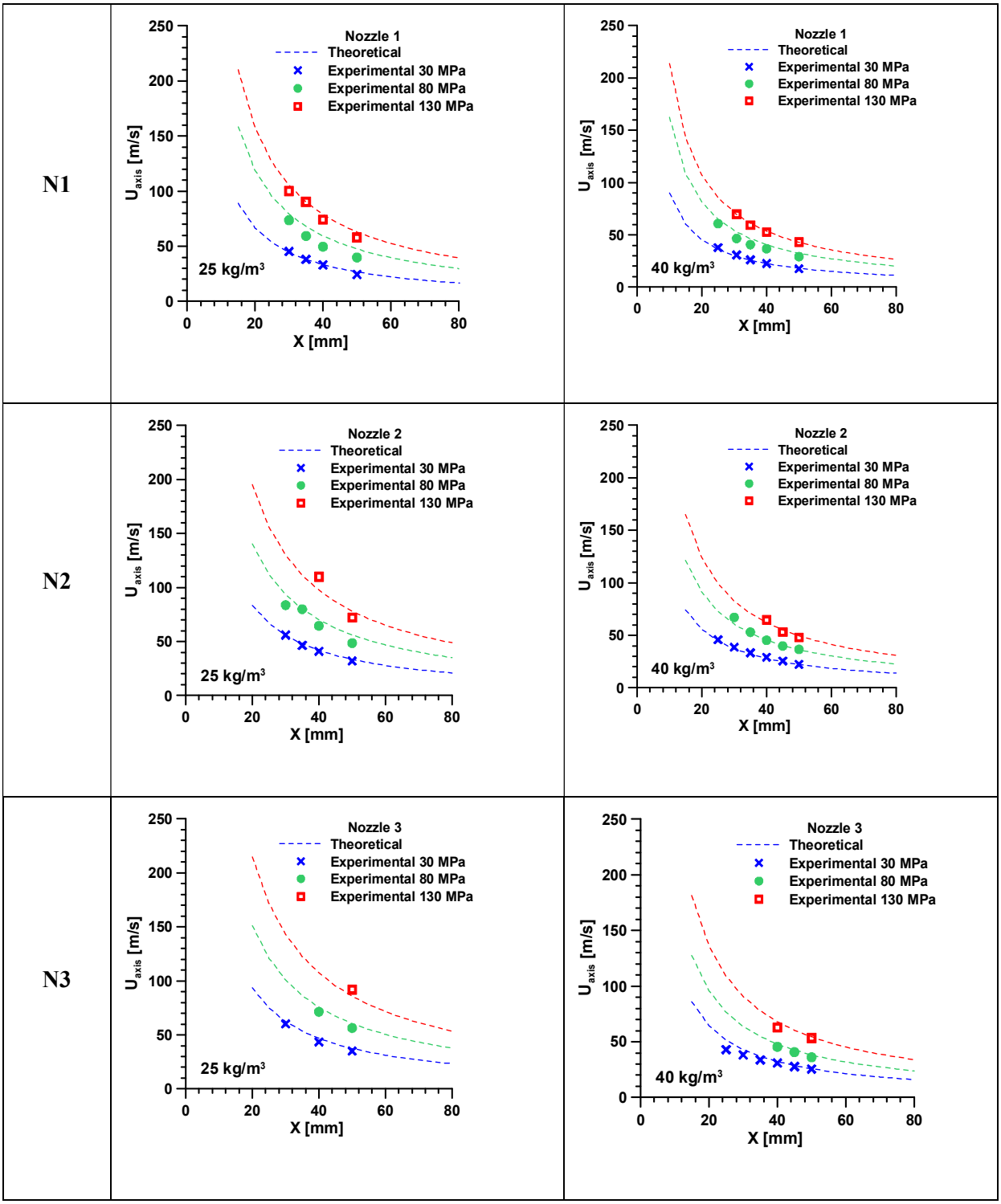

Figure 5. On-axis velocity measurements for all nozzles at a different injection conditions. Comparison between experimental measurements and model.